Abaqus Simulation of the Fire's Impact on Reinforced Concrete Bubble Deck Slabs

Ahmed A. Al-Ansari[1, a*], Majid M. Kharnoob[1,b] and Mustafa A. Kadhim[2, c]

[1]Department of Civil Engineering, University of Baghdad, Baghdad, Iraq

[2]Department of Engineering, University of Karbala, Karbala, Iraq

[a]Ahmed.ibrahim2001m@coeng.uobaghdad.edu.iq , [b]dr.majidkharnoob@coeng.uobaghdad.edu.iq and

[c]mustafa.amoori@s.uokerbala.edu.iq

*Corresponding author

Abstract. The use of Bubble Deck in modern prefabricated construction methods has recently become widespread in industrial projects worldwide. In the middle of a typical slab, Bubble Deck places hollow plastic balls that do not improve structural performance but significantly reduce structural weight. This study analyzes the behavior of self-uniting bidirectional concrete slabs with plastic spherical voids under high temperatures and for different periods. Six simply supported bidirectional plates, five of which contained bubbles and one solid, were numerically tested using the finite element method and the commercial ABAQUS software to investigate the behavior of bidirectional plates fired at various temperatures and for various amounts of time. Each slab has the following measurements: (1500*1500*150) mm. These slabs were fired at different temperatures (600 and 800) °C and for different periods (one and two hours). The slabs were classified into four groups depending on the kind of slab (solid or bubble), the degree of burning (600 and 800) °C, and the duration of the burning (one and two hours). The loading strength of concrete was found to be up to 65% less than the maximum capacity of a slab that was bubbled and fired at high temperatures. The length of the firing time also had a significant effect on reducing the strength of the concrete. The longer the firing period, the lower the load resistance of the concrete. The ball would melt and scorch in an intense, protracted fire without noticeable effects. The ability of the steel to maintain adequate strength during a fire, when it will be burned and lose significant strength as the temperature rises, determines the slab's ability to withstand fire. Bubble deck slabs produce between 17% and 39% stronger thermal resistance than an equivalent solid slab of the same depth, even though they are not intended to provide thermal insulation due to the encapsulation of the air bubbles within the center of the concrete slab.

Keywords: Two-way slabs; fire flame; hollow plastic spheres; burn duration; flexural failure; finite element analysis.

1. INTRODUCTION

Plastic spheres in RC (reinforced concrete) two-way slabs are one of the most modern methods for making slabs lighter. Due to an up to 35% decrease in self-weight, an increase in slab span, and a decrease in the overall cost of the structure, by using fewer materials, carbon emissions from apparatus use and transportation will also be reduced. The consumption bubbles can also be recycled or saved for other endeavors [1]. Compared to conventional concrete slabs, bubble deck slabs have many advantages, including less material consumption, lower overall costs, efficiency, quicker building times, and being a green technology Mushfiq et al. [2]. This type of slab is known as a bubbling slab system. This technique is widely used in Europe. Owing to the plastic bubbles' existence, which significantly reduces shear strength by removing a portion of the concrete, the decrease factor for the shear capacity of the bubbled slab is equal to (0.6) that of the solid slab [3]. Because of this, it is advised to eliminate the bubbles surrounding the columns, as seen in Figure 1 [4]. The flexural and shear behavior of the bubbled slabs was investigated through several studies and experiments. Al-Rashedi and Al-Ahmed [5] used post-tensioned pre-stressed strands to reduce deflection and improve slab capacity when long spans are necessary. Because of the smaller area of the cross-section that spherical voids provide, Al-Rashedi asserts that voids positioned below the neutral axis of the slab (in the tension zone), obtained the same strength as solid slabs with 10–20% Saifee and Parikh (6) used SAP 2000 to do an analytical evaluation of solid flat slabs and voids in 2014. The models' sizes vary from (6 x 6 m) to (14 x 14 m), with slab thicknesses ranging from 280 to 600 mm and the hollow void former's diameter from 180 to 450 mm. Voided slabs are modeled in the same way as solid slabs. According to the test results, the voided slabs are less stiff than the solid slabs. In addition, adding voids to the slabs can lower their self-weight by as much as 32%.

The slab modeling revealed the position of the highest positive moment for both voided and solid slabs. Since fire is one of the most hazardous environmental situations to which buildings may be exposed, it demands special consideration that suitable fire safety measures are provided for structural components. Building and structure fires can result in both material and human losses. Recent studies have concentrated on figuring out how to design fire-resistant structures and fortify buildings against fires (Gravit and Dmitriev

2022, Tlidji et al. 2021) [7] They investigated how the ISO 834-compliant fire conditions affected the behavior of CFRP-coated steel beams coated in gypsum-based mortar. Dual finite element analyses of 3D temperature and displacement were conducted to examine the effectiveness of these beams. Alim Al Ayub Ahmed et al. [8] used the adhesion model to simulate the interaction between the steel sheet and carbon fiber-reinforced plastic. Analysis was done on the impact of temperature, CFRP panel strength, and fire-retardant coating thickness on the deformation of beams. According to the findings, the highest temperature of the steel beam's outer surface was decreased from 380°C to 270°C during the first 120 minutes of fire exposure by increasing the thickness of the fire-retardant coating from 1 mm to 10 mm. This 30% reduction in the rate of temperature development of the steel beam was made possible by thickening the fireproof coating. The suggested fireproof coating approach and gypsum-based mortar, which can be applied to building materials, can offer higher fire protection for the Bubble Deck slab besides the outstanding thermal resistance. In the course of a fire, several structural components are subjected to different heat stress distributions, which can result in significant deformations and buckling. Therefore, looking at how well structures withstand fire and offer workable methods to enhance that performance is essential. Steel buildings can sustain structural damage during and after a fire, much like other building materials. Steel loses a substantial amount of its strength and stiffness at high temperatures. The effect of fire conditions according to an iso834 standard on the behavior of reinforced steel. The result is within the first 120 minutes of five exposures [9].

The main objective of this research is to verify the behavior of the bubble surface panels for fire resistance, where all the panels will be exposed to fire flame for different periods and at high temperatures using the FEM program.

Figure 1: Bubbled slab system [10].

2. PROPOSED SLAB MODELS AND SPECIMEN DETAILS

In this article, six proposed models of the two-way RC panel were tested. These panels had recommended sizes of (1500 x 1500 x 150) mm. It also has plastic balls with a diameter of (120) mm. They are divided into four groups according to the degree of burning (600 and 800) °C and the duration of burning (one and two hours). The first and second groups were divided based on the severity of burning, while the third and fourth groups were divided based on the duration of burning. The designations and details of the proposed panels can be found in Table 1. The main layer was designed with reinforcing steel with a diameter of 6 mm in both directions (the distances between the reinforcing steel as shown in Figure 2) depending on the location of the sphere. The secondary layer was reinforced with reinforcing steel with a diameter of 4 mm in both directions, and the distances between the reinforcing steel were the same as the distances of the main layer. The steel reinforcement used in the simulation study was plain reinforcement type. An embedded region constraint was used to simulate the full interaction bond between the concrete slab and steel reinforcement to overcome the deformations in the steel bar.

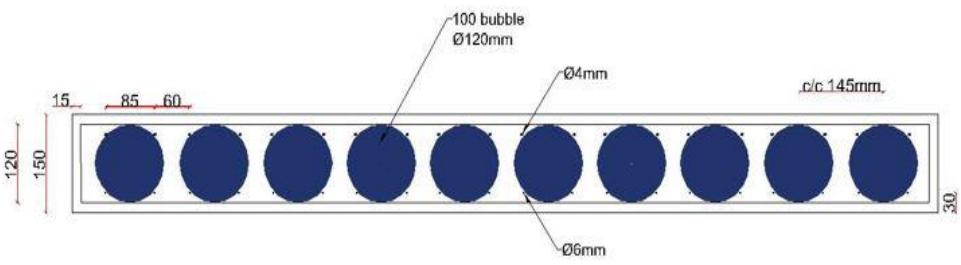

Figure 2: Proposed slab model.

3. SPECIMEN MODELING IN THE ABAQUS SOFTWARE

Four proposed combinations of simply supported two-way (RC) plates are performed in a finite element analysis (FEA) using the computer software ABAQUS. As mentioned earlier, each group consists of four modular models. The four groups were divided according to the degree of burning and the duration of burning. In the first and second groups, the temperature and combustion period will be constant. As for the third and fourth groups, the burning period will be constant, and the temperature will be variable. Plastic balls were placed inside the models. The diameter of the ball is 12 cm to reduce the weight. The reinforcing steel rests directly on the balls without needing chairs, as shown in in Figure 3. The model was also reinforced with two networks of reinforcing steel, upper and lower, with a diameter of 4 mm and 6 mm, respectively. One hundred balls were distributed inside each model at equal distances between them and spread on all parts of the model. High heat was applied to all four sides of the model and from the bottom of the model. The thermal distribution of the numerical models of the RC slab is not equal because the heat is directed from the sides and the bottom only and not from all directions, as the temperature will be high in places close to the flame and gradually decrease as we move away from the source of the fire. The concrete cover prevents part of the heat, so we see that the lowest temperature is in the core of the concrete Figure 4. These panels are analytically subjected to a concentrated load in the middle applied to a steel plate to withstand high loads with dimensions (200 *200*20) mm. The load is applied until failure.

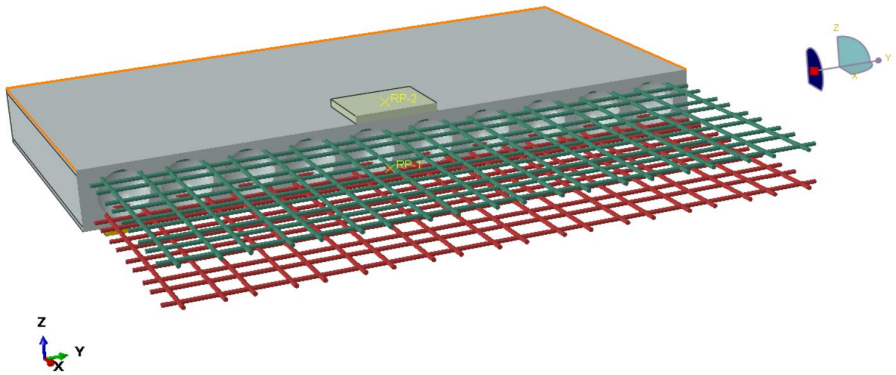

Figure 3: Slab models and distribution of bubble in the slab.

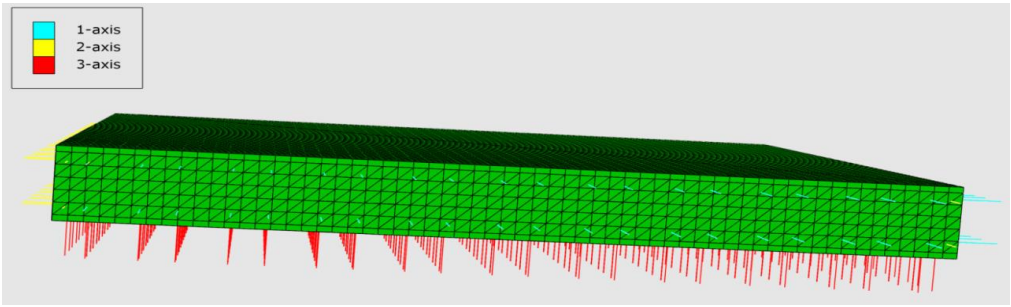

Figure 4: Direction of fire.

3.1 Numerical Simulation in ABAQUS

1) Geometric modeling (3D deformable object for concrete slab, wire element 1D for steel reinforcement, rigid body for supporting plate (nondeformable). The bubbles were created in and copied in two dimensions and then extracted from the main slab concrete in the assembly using the merge/ cut instance tool.
2) Material characterization for concrete and steel (CDP model for concrete behavior, elastic, perfect plastic for steel reinforcement) as a function of temperature. The length of the fire exposure, the method of cooling, and the kind of skeleton materials all impacted the concrete's post-fire mechanical properties. Here, Yu et al. [11,12] post-fire concrete model was applied. The post-fire concrete's compression stress-strain model (Figure 5) can be calculated using formulas 2 and 3. According to formula 1, Figure 6 illustrates the axial compressive strength of concrete's reduction factor with temperature variation. The post-fire concrete's strength loss factor at T°C is:

$$\Psi cT = \frac{fc(T)}{fc} = \frac{1}{1 + 9 \times [(T - 20)/800]c1} \quad (1)$$

where fc(T) denotes the concrete's axial compressive strength at a high temperature. N/mm²; fc is the concrete's axial compressive strength at room temperature, N/mm². The parameter is c1 in this case is 3.55 for regular concrete), Concrete c1 = 6.70 for high-performance concrete (HPC). For high-performance concrete (HPC) concrete c1 = 6.70.

Post-fire concrete's compression peak strain ε_0(T) at T°C is:

$$\varepsilon_0(T) = \{1 + c_4[(T - 20)/100]^2\}\,\varepsilon_0 \quad (2)$$

where ε_0 represents the concrete's compressive strain at room temperature. The parameter is c4, which in this case is 0.037 for ordinary concrete. In the case of high-performance concrete (HPC), c_4 = 0.017. After a fire, concrete's compression stress-strain relationship can be stated as

$$y = \begin{cases} \dfrac{9.1 f_{cu}^{-4/9} x - x^2}{1 + \left(9.1 f_{cu}^{-4/9} - 2\right)x} & x \le 1 \\ \dfrac{x}{2.5 \times 10^{-5} f_{cu}^{3} (x-1)^2 + x} & x > 1 \end{cases} \quad (3)$$

where y = σc/fc(T), x = εc/ε0(T), σc is the compressive stress of post-fire concrete, N/mm²; ε_C is the post-fire concrete's compressive strain, and fcu is the cube crushing strain.

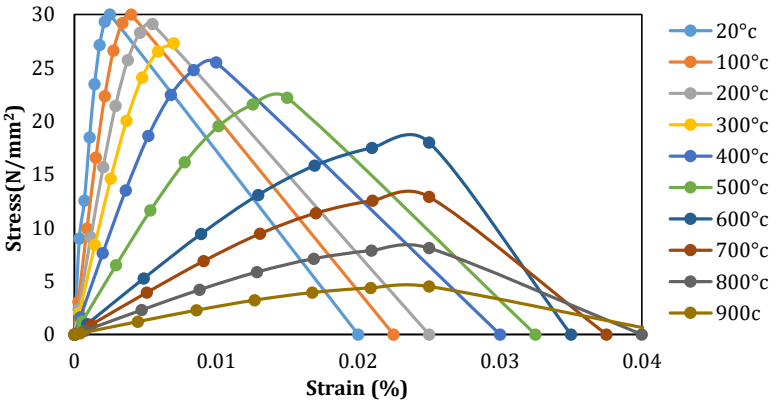

Figure 5: Stress-strain curves of concrete at different temperatures [11,12].

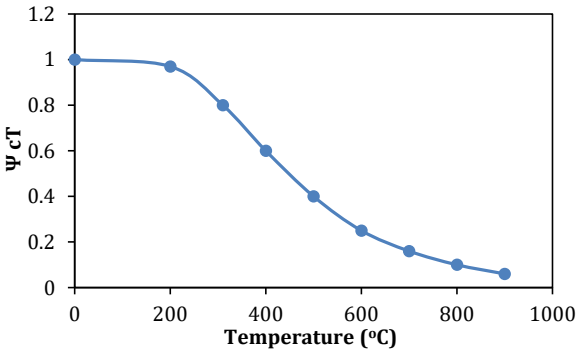

Figure 6: Reduction factor of concrete compressive strength [11,12]

ABAQUS' integrated bilinear kinematic reinforcement model simulated reinforcement steel, and the elastic modulus Es(T) (N/mm²) at T °C proposed by Yu et al. [11,12] can be determined using the following formula.

$$\frac{E_s(T)}{E_s} = \begin{cases} 1 & \le 350°C \\ 1.0072 - 2.014 \times 10^{-7} T^2 + 5 \times 10^{-5} T & > 350°C \end{cases} \quad (4)$$

concrete's tensile strength at room temperature, N/mm2. The concrete's post-fire elastic modulus Ec (T) (N/mm²) at T °C is

$$E_c(T) = \frac{E_c}{1+2.15\times10^{-3}[(T-20)/800]^{4.33}+3.7\times10^{-2}[(T-20)/100]^2} \quad (5)$$

where Es is the elastic modulus of reinforcement at room temperature, N/mm². The yield strength reduction factor of reinforcement ΨyT at T °C proposed by Miao et al. [13] is as follows:

$$\psi_{yT} = \frac{f_y(T)}{f_y} = \begin{cases} 1 & 0℃ < T \le 200\,℃ \\ 1.33-1.64\times10^{-3}T & 200℃<T\le700\ \ ℃ \end{cases} \quad (6)$$

where fy (T) is the reinforcement's post-fire yield strength, N/mm²; fy stands for the reinforcement's yield strength at room temperature, N/mm².The following is a representation of the stress-strain model for reinforcing at high temperature (Figure 7).

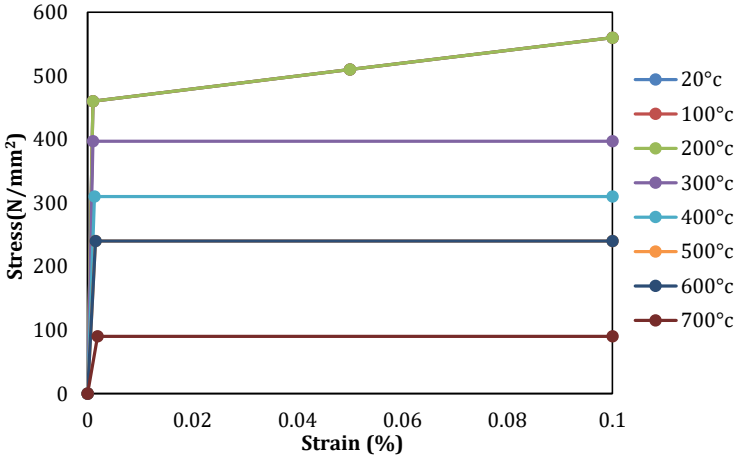

Figure 7: Stress-strain curves of steel at elevated temperature [11,12].

3) Mesh (steel, concrete), element type, and boundary condition.
4) Constrain and interaction (embedded region constrain (between steel and concrete)), interaction 2 (heat transfer using convection method by utilizing the surface film condition and ISO 874 the temperature-time curve was defined in this interaction), and surface-to-surface contact (normal and tangential contact type) to simulate the interaction between concrete body and the steel supporting plate.
5) Loading protocol (1- thermal analysis using thermal analysis in ABAQUS without mechanical loading to simulate the thermal loading), step 2 (temperature-displacement analysis) involves recalling the heated model as an initial condition to the mechanical loading model and displacement control method was adopted to simulate such type of loading.
6) Mesh and element type.

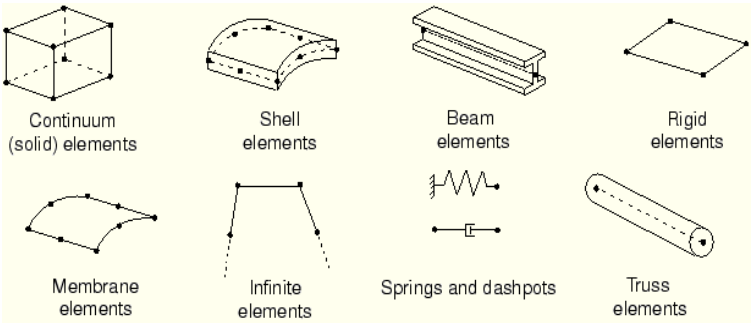

Figure 8: Geometric modeling.

3.2 Selected Fire Amplitude

A heating curve was used as the foundation for the heat transfer study. The International Organization's (ISO 1999) ISO-834 [2] fire curve is used here (Figure 9). The equation of the curve can be written as [14,15].

$$T = T_0 + 345\log_g(8t+1) \quad (7)$$

where t is the heating time in minutes and T0 is the starting temperature, which in this case is 20°C.

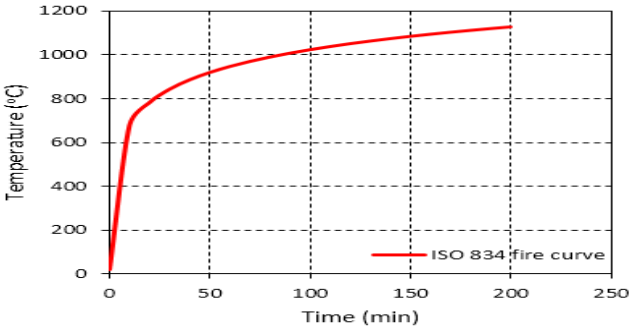

Figure 9: ISO-834 fire curve.[9]

4. FINITE ELEMENT ANALYSIS RESULTS

4.1 Ultimate Load Capacity

The slabs were designed and analyzed using finite element analysis software, and these results are shown in Table 1. Table 1 presents the results of the final slab load and deflection capacity tests performed numerically using FEA software (ABAQUS). The effect of high temperature also appears on the panels, as the loading decreases with the increase in temperature. Likewise, the loading strength decreases as the firing period increases. The loading force is reduced by 13% for plates containing plastic balls compared to plates without plastic balls (SD1 and BD1). The slabs were designed and analyzed using finite element analysis software, and these results are shown in Table 1. When analyzing the slabs in the Finite Element Program, the results were as follows:

a) In the first group, the samples were fired at a temperature of(600°C) in two different periods (1 hour and 2 hours). It was found that the loading strength decreased by 30% when burning the slab at a temperature of (600°C) for one hour and when burning the second sample at a temperature of 600 for two hours. It's noted that the load force decreased by 52% of the load force before burning.
b) In the second group, the temperature was raised to 800°C (for one hour and two hours), and it was found that the loading force decreased by 40% of the original loading strength. When the burning time was increased to two hours, it was found that the loading force decreased by 65% of the original loading force.
c) In the third group, the time will be an hour, and the temperature (800 and 600) °C, the load strength at a temperature of 800°C will decrease by 15% compared to the load strength at a temperature of 600°C
d) As for the fourth group, the burning period will be two hours, and we note that the loading force at a temperature of 800°C decreased by 35% compared to the loading strength at a temperature of 600°C. This confirms that the burning period has a more negative effect on the slabs than the high-temperature

Table 1. Maximum load capability and maximum deflection.

Group	Design specimen	Type of Specimen	Number of Bubbles	Bubble Diameter (mm)	Weight reduction (%)	Ultimate load (kN)	Ultimate deflection (mm)	burn degree (°C)	burn duration (hr)
I	SD1	solid	0	0	0	271	38.5	0	0
	BD1	bubbled	100	12	27	235	25.6	0	0
	BD2	bubbled	100	12	27	167.5	25.6	600	1
	BD3	bubbled	100	12	27	112.4	25.6	600	2
II	SD1	solid	0	0	0	271	38.5	0	0
	BD1	bubbled	100	12	27	235	25.6	0	0
	BD4	bubbled	100	12	27	143	25.7	800	1
	BD5	bubbled	100	12	27	81.8	25.7	800	2
III	SD1	solid	0	0	0	271	38.5	0	0
	BD1	bubbled	100	12	27	235	25.6	0	0
	BD2	bubbled	100	12	27	167.5	25.6	600	1
	BD4	bubbled	100	12	27	143	25.7	800	1
IV	SD1	solid	0	0	0	271	38.5	0	0
	BD1	bubbled	100	12	27	235	25.6	0	0
	BD3	bubbled	100	12	27	112.4	25.6	600	2
	BD5	bubbled	100	12	27	81.8	25.7	800	2

4.2 Deflection Response to Load

Reading of deflections in the center of the slab and showing how the slabs will behave, load-deflection curves are drawn when the slabs are fired at different temperatures and for different periods, as shown in **Figure 10.** Temperature affects the loading strength of the slabs. As the loading strength decreases with increasing temperature, it decreases by 40% when heating at 800ºC for one hour, and time also significantly affects the loading strength as the loading strength decreases by 65% of the original bearing strength when burning at 800ºC for Two hours. Plastic balls affect the deflection, as the deflection in ordinary concrete is about 38 mm, while the deflection in concrete containing plastic balls is 25 mm. High temperatures do not affect the deflections of the ball plates, but only the bearing strength. The following conclusions are made after examining the failure modes of the examples shown in Figure 11: Flexure failure will be the predominant failure mode for all slab models. The cracks are represented by a green area that radiates outward horizontally from the center toward the corner.

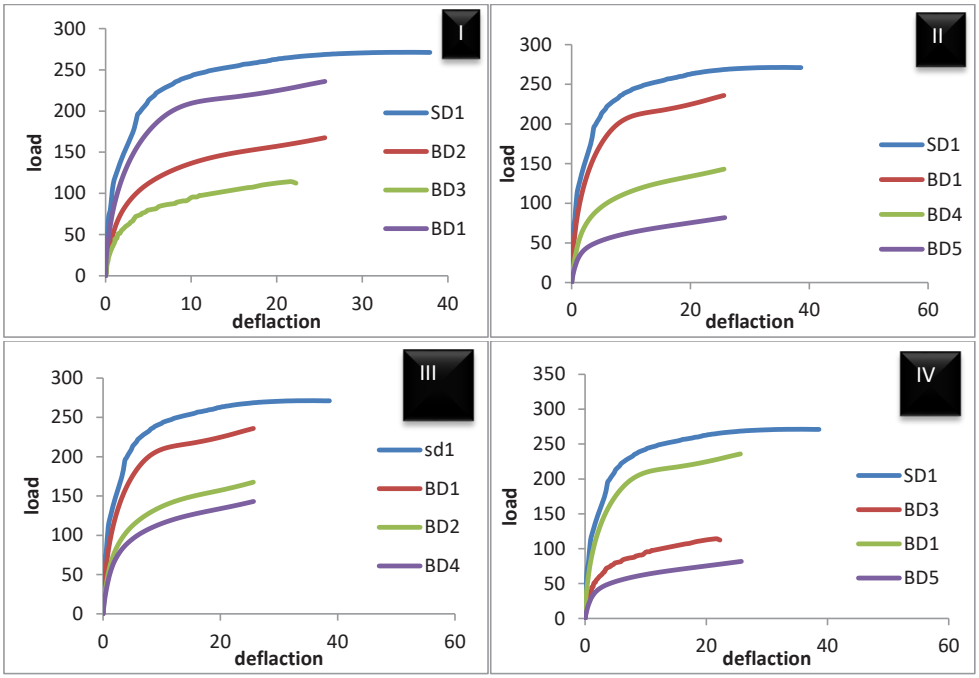

Figure 10: Load-deflection response.

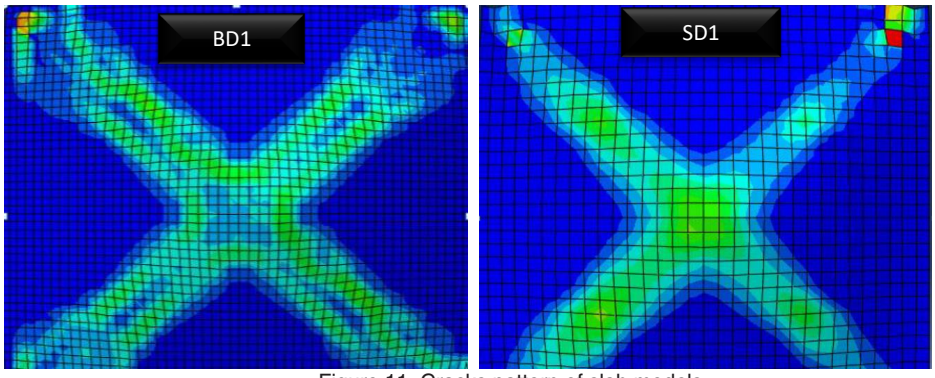

Figure 11: Cracks pattern of slab models.

4.3 Thermal Distribution of Slabs

Temperatures are gradually distributed from the outer layers to the inner layers and from areas close to the flame to areas far from the flame, where the greatest concentration is on the edges, then the far areas, and it is less in the core of the slab. The thermal distribution of the slab is uneven because the flame sources are present in the sides only and not in all directions. Therefore, the heat is strong at the ends and gradually decreases as we move away from the source of the flame. The slabs were not directly exposed to the flame

of fire, but the air surrounding the slabs was heated, which in turn heated the models. Figures 12 and 13 show the heat distribution of the models, where we notice that the edges close to the flame have a very high temperature, and the temperature decreases as we move away from the flame source.

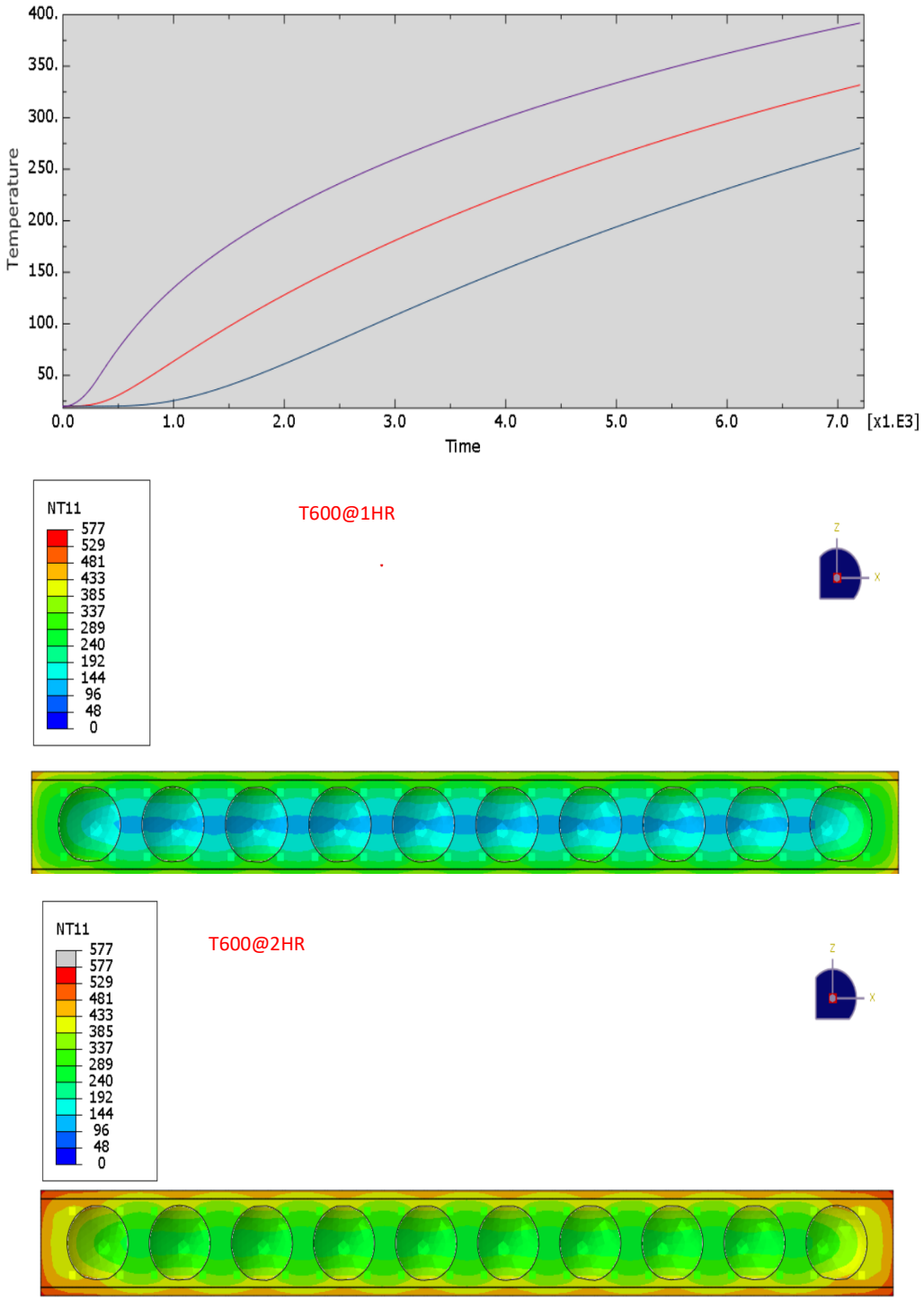

Figure 12: Thermal distribution of slabs (600°C).

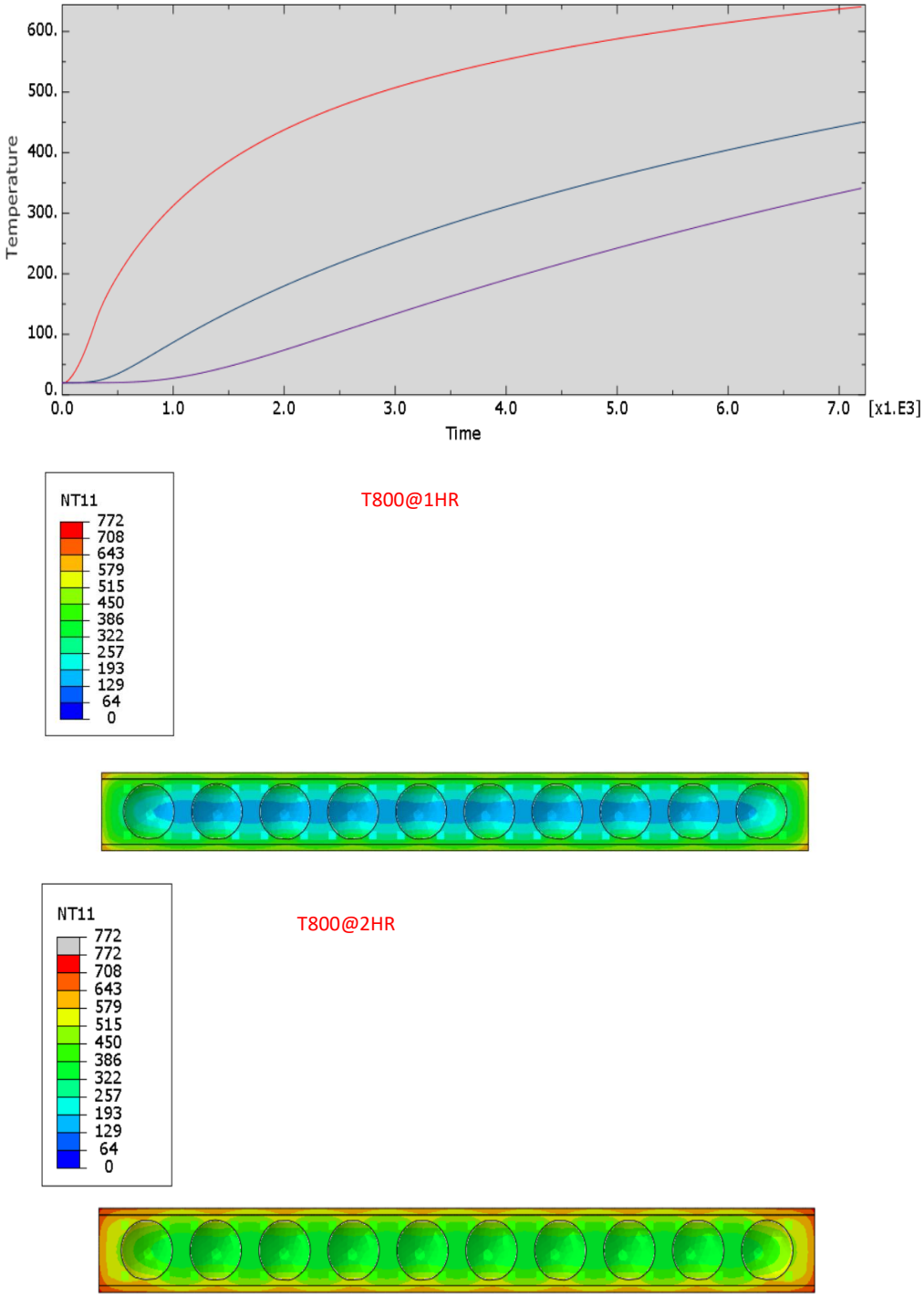

Figure 13: Thermal distribution of slabs (800°C).

5. SUMMARY AND CONCLUSIONS

From this research's analytical results, the following inferences can be drawn:

- The ABAQUS Sequential Thermo-mechanical coupling model can accurately replicate the bubble deck slab.

- Compared to a normal solid slab, the weight of the bubbled slabs with a bubble diameter to slab thickness ratio (D/H) of 0.80 can be lowered by 27%.
- With D/H ratios of (0.80), bubbled slabs can sustain (85%) of the maximum load compared to the reference solid slab.
- Compared to the reference bubble slab, the loading force is 30% lower when burning a sample at 600°C for one hour.
- Compared with the reference bubble sheet, the loading strength is 30% lower when burning a sample at 600°C for 1 hour, 40% when burning a sample at 800°C for 1 hour, and 47% when burning a sample at 600°C for 2 hours, and 65% when burning a sample at 800°C for two hours.
- The firing duration affects the loading resistance relatively more than the temperature rise for a shorter period, as the loading strength decreased when burning the model for two hours at a temperature of 600°C more than when burning the model for one hour at a temperature of 800°C.
- The direction of failure is similar in all models, starting from the middle and heading towards the edges in the form of the letter X, as in Figure 7.
- The temperature only affects the bearing strength of the concrete and does not affect the deflection except by a very small percentage.
- After a prolonged period of fire exposure, the flexural capacity was drastically reduced.
- The ball would melt and finally scorch in an intense, protracted fire without having any noticeable effects.
- Bubble deck slabs produce between 17% and 39% stronger thermal resistance than an equivalent solid slab of the same depth, even though they are not intended to provide thermal insulation due to the encapsulation of the air bubbles within the center of the concrete slab.
- Concrete's ability to withstand fire for roughly 60 to 180 minutes.

REFERENCES

[1] Building Code Requirements for Structural Concrete, 318, 2019.
[2] M.S. Mushfiq, S. Saini, N. Rajoria,(Experimental Study on Bubble Deck Slab): (2017).submitted to International Research Journal of Engineering and Technology (IRJET).
[3] Bubble Deck UK. (2006, Apr.), Properties of BubbleDeck Slab, details regarding: http://www.BubbleDeck-UK.com
[4] C.J. Midkiff, (Plastic Voided Slab System Application and Design). (2013) M.Sc. thesis, Dept. Arch. Eng., Kansas State Univ., Kansas State, USA,.
[5] Qazani, M.R.C., Asadi, H., Khoo, S. and Nahavandi, S., (A linear time-varying model predictive control-based motion cueing algorithm for hexapod simulation-based motion platform), (2019), IEEE Trans. Syst. Man Cybernet.: Syst., 51(10), 6096-6110. https://doi.org/10.1109/TSMC.2019.2958062.
[6] Saifee Bhagat and Parikh, K. B., (Comparative Study of Voided Flat Plate Slab and Solid Flat Plate Slab), (2014), International Journal of Innovative Research and Development, March Vol. 3, Issue 3,.
[7] Gravit, M. and Dmitriev, I.,(Light steel framing with mineral wool fire protection under fire exposure), (2022), Proceedings of MPCPE 2021, 247-257
[8] Alim A. A. and Majid M.kharnoob,(Flexural response of steel beams strengthened by fiber-reinforced plastic plate and fire retardant coating at elevated temperatures), (2022), Structural Engineering and Mechanics, Vol. 83, No. 4 (2022) 551-561
[9] ISO 834-1:1999 (International Organisation for Standardisation) Fire resistance tests-Elements of building construction. Part 1: General requirements. Geneva: ISO
[10] Yu, Ding, F. X., Z. W., & Luo, J. P. (Experimental research on mechanical properties of different type of concrete after high temperature)(2005). Journal of Safety and Environment, 5(5), 1–6.
[11] Yu, Z. Q., Wang, Z. W., & Shi, Z. F.(Experimental research on material properties of new three-grade steel bars after fire). (2005). Journal of Building Structures, 26(02), 112–116.
[12] Miao, Chen, Hou, J. J, N., X. Y., Q. Q., Zhu, & Gong, (W. Experimental research and numerical simulation on fire resistance performance of RC beams with damages caused by service loading) (2013). Journal of Building Structures, 34(03), 1–11.
[13] Butterworth- Heinemann (Design and Analysis of Tall and Complex Structures) (2018)., ELSEVIER, ISBN 978-0-08-101121-8.
[14] Fu, F. Structural analysis and design to prevent disproportionate collapse. (2016), CRC Press ISBN 978-1-4987-8820-5.